AD-A197 019

OFFICE OF NAVAL RESEARCH

Technical Report #23

Bis(Dioxolene)(Bipyridine)Ruthenium Redox Series

By

A.B.P. Lever*, Pamela R. Auburn, Elaine S. Dodsworth, Masa-aki Haga,
Wei Liu, Milan Melnik and W. Andrew Nevin

in

Journal of American Chemical Society

York University
Department of Chemistry, 4700 Keele St., North York
Ontario, Canada M3J 1P3

88

REPORT DOCUMENTATION PAGE

1a. REPORT SECURITY CLASSIFICATION		1b. RESTRICTIVE MARKINGS			
2a. SECURITY CLASSIFICATION AUTHORITY Unclassified		3. DISTRIBUTION/AVAILABILITY OF REPORT As it appears on the report			
2b. DECLASSIFICATION/DOWNGRADING SCHEDULE					
4. PERFORMING ORGANIZATION REPORT NUMBER(S) Report #23		5. MONITORING ORGANIZATION REPORT NUMBER(S)			
6a. NAME OF PERFORMING ORGANIZATION A.B.P. Lever, York University Chemistry Department	6b. OFFICE SYMBOL (If applicable)	7a. NAME OF MONITORING ORGANIZATION Office of Naval Research			
6c. ADDRESS (City, State, and ZIP Code) 4700 Keele St., North York, Ontario M3J 1P3 Canada		7b. ADDRESS (City, State, and ZIP Code) Chemistry Division 800 N. Quincy Street Arlington, VA 22217 U.S.A.			
8a. NAME OF FUNDING/SPONSORING ORGANIZATION	8b. OFFICE SYMBOL (If applicable)	9. PROCUREMENT INSTRUMENT IDENTIFICATION NUMBER N00014-84-G-0201			
8c. ADDRESS (City, State, and ZIP Code)		10. SOURCE OF FUNDING NUMBERS			
		PROGRAM ELEMENT NO.	PROJECT NO.	TASK NO.	WORK UNIT ACCESSION NO

11. TITLE (Include Security Classification)

Bix(Dioxolene)(Bipyridine)Ruthenium Redox Series

12. PERSONAL AUTHOR(S) A.B.P. Lever*, Pamela R. Auburn, Elaine S. Dodsworth, Masa-aki Haga, Wei Liu, Milan Melnik and W. Andrew Nevin

13a. TYPE OF REPORT Technical	13b. TIME COVERED FROM Aug. 87 TO Aug. 88	14. DATE OF REPORT (Year, Month, Day) July 11, 1988	15. PAGE COUNT 49

16. SUPPLEMENTARY NOTATION

17	COSATI CODES		18. SUBJECT TERMS (Continue on reverse if necessary and identify by block number)
FIELD	GROUP	SUB-GROUP	Quinone, Ruthenium, Delocalisation, Redox Series,

19. ABSTRACT (Continue on reverse if necessary and identify by block number)

Complexes of the general formula $[Ru(bpy)(dioxolene)_2]^{n+}$ have been prepared where (bpy) is 2,2'-bipyridine, and n = -1,0,+1. The dioxolene ligand is 1,2-dihydroxybenzene (catechol), 3,5-di-t-butyl- or 3,4,5,6-tetrachloro-1,2-dihydroxybenzene which may formally exist in the catecholate, semiquinone or quinone oxidation state. Redox series of up to five members have been prepared by controlled potential electrolysis of the parent species or, in some cases, by chemical oxidation or reduction. Electrochemistry, magnetism, X-ray structural data and ultraviolet, visible and near infrared electronic, resonance Raman, vibrational (FTIR), nuclear magnetic resonance, electron spin resonance and photoelectron spectra, for various members of the redox series, are discussed in terms of the electronic structures (effective oxidation states, delocalization) of the complexes. Apparent conflicts between results obtained using different techniques are resolved using a simple, qualitative MO model.

20. DISTRIBUTION/AVAILABILITY OF ABSTRACT ☒ UNCLASSIFIED/UNLIMITED ☐ SAME AS RPT ☐ DTIC USERS	21. ABSTRACT SECURITY CLASSIFICATION Unclassified/unlimited	
22a. NAME OF RESPONSIBLE INDIVIDUAL Dr. Robert K. Grasselli	22b. TELEPHONE (Include Area Code)	22c. OFFICE SYMBOL

TECHNICAL REPORT DISTRIBUTION LIST, GEN

	No. Copies		No. Copies
Office of Naval Research Attn: Code 1113 800 N. Quincy Street Arlington, Virginia 22217-5000	2	Dr. David Young Code 334 NORDA NSTL, Mississippi 39529	1
Dr. Bernard Douda Naval Weapons Support Center Code 50C Crane, Indiana 47522-5050	1	Naval Weapons Center Attn: Dr. Ron Atkins Chemistry Division China Lake, California 93555	1
Naval Civil Engineering Laboratory Attn: Dr. R. W. Drisko, Code L52 Port Hueneme, California 93401	1	Scientific Advisor Commandant of the Marine Corps Code RD-1 Washington, D.C. 20380	1
Defense Technical Information Center Building 5, Cameron Station Alexandria, Virginia 22314	12 high quality	U.S. Army Research Office Attn: CRD-AA-IP P.O. Box 12211 Research Triangle Park, NC 27709	1
DTNSRDC Attn: Dr. H. Singerman Applied Chemistry Division Annapolis, Maryland 21401	1	Mr. John Boyle Materials Branch Naval Ship Engineering Center Philadelphia, Pennsylvania 19112	1
Dr. William Tolles Superintendent Chemistry Division, Code 6100 Naval Research Laboratory Washington, D.C. 20375-5000	1	Naval Ocean Systems Center Attn: Dr. S. Yamamoto Marine Sciences Division San Diego, California 91232	1

DTIC
COPY
INSPECTED
6

Accession For

NTIS CRA&I	☒
DTIC TAB	☐
Unannounced	☐
Justification	

By

Distribution/

Availability Codes

Dist	Avail and/or Special
A-1	

ABSTRACTS DISTRIBUTION LIST,359/627

Dr. Manfred Breiter
Institut fur Technische Elektrochemie
Technischen Universitat Wien
9 Getreidemarkt, 1160 Wien
AUSTRIA

Dr. E. Yeager
Department of Chemistry
Case Western Reserve University
Cleveland, Ohio 44106

Dr. R. Sutula
The Electrochemistry Branch
Naval Surface Weapons Center
Silver Spring, Maryland 20910

Dr. R. A. Marcus
Department of Chemistry
California Institute of Technology
Pasadena, California 91125

Dr. J. J. Auborn
AT&T Bell Laboratories
600 Mountain Avenue
Murray Hill, New Jersey 07974

Dr. M. S. Wrighton
Chemistry Department
Massachusetts Institute
 of Technology
Cambridge, Massachusetts 02139

Dr. B. Stanley Pons
Department of Chemistry
University of Utah
Salt Lake City, Utah 84112

Dr. Bernard Spielvogel
U.S. Army Research Office
P.O. Box 12211
Research Triangle Park, NC 27709

Dr. Mel Miles
Code 3852
Naval Weapons Center
China Lake, California 93555

Dr. P. P. Schmidt
Department of Chemistry
Oakland University
Rochester, Michigan 48063

Dr. Roger Belt
Litton Industries Inc.
Airtron Division
Morris Plains, NJ 07950

Dr. Ulrich Stimming
Department of Chemical Engineering
Columbia University
New York, NY 10027

Dr. Royce W. Murray
Department of Chemistry
University of North Carolina
Chapel Hill, North Carolina 27514

Dr. Michael J. Weaver
Department of Chemistry
Purdue University
West Lafayette, Indiana 47907

Dr. R. David Rauh
EIC Laboratories, Inc.
Norwood, Massachusetts 02062

Dr. Edward M. Eyring
Department of Chemistry
University of Utah
Salt Lake City, UT 84112

Dr. M. M. Nicholson
Electronics Research Center
Rockwell International
3370 Miraloma Avenue
Anaheim, California

Dr. Nathan Lewis
Department of Chemistry
Stanford University
Stanford, California 94305

Dr. Hector D. Abruna
Department of Chemistry
Cornell University
Ithaca, New York 14853

Dr. A. B. P. Lever
Chemistry Department
York University
Downsview, Ontario M3J 1P3

ABSTRACTS DISTRIBUTION LIST, 359/627

Dr. Martin Fleischmann
Department of Chemistry
University of Southampton
Southampton SO9 5H UNITED KINGDOM

Dr. Alan Bewick
Department of Chemistry
The University of Southampton
Southampton, SO9 5NH UNITED KINGDOM

Dr. John Wilkes
Department of the Air Force
United States Air Force Academy
Colorado Springs, Colorado 80840-6528

Dr. Edward Fletcher
Department of Mechanical Engineering
University of Minnesota
Minneapolis, Minnesota 55455

Dr. R. A. Osteryoung
Department of Chemistry
State University of New York
Buffalo, New York 14214

Dr. Bruce Dunn
Department of Engineering &
   Applied Science
University of California
Los Angeles, California 90024

Dr. Janet Osteryoung
Department of Chemistry
State University of New York
Buffalo, New York 14214

Dr. Elton Cairns
Energy & Environment Division
Lawrence Berkeley Laboratory
University of California
Berkeley, California 94720

Dr. A. J. Bard
Department of Chemistry
University of Texas
Austin, Texas 78712

Dr. Richard Pollard
Department of Chemical Engineering
University of Houston
Houston, Texas 77004

Dr. Steven Greenbaum
Department of Physics and Astronomy
Hunter College
695 Park Avenue
New York, New York 10021

Dr. M. Philpott
IBM Research Division
Mail Stop K 33/801
San Jose, California 95130-6099

Dr. Donald Sandstrom
Boeing Aerospace Co.
P.O. Box 3999
Seattle, Washington 98124

Dr. Martha Greenblatt
Department of Chemistry, P.O. Box 939
Rutgers University
Piscataway, New Jersey 08855-0939

Mr. James R. Moden
Naval Underwater Systems Center
Code 3632
Newport, Rhode Island 02840

Dr. Anthony Sammells
Eltron Research Inc.
4260 Westbrook Drive, Suite 111
Aurora, Illinois 60505

Dr. D. Rolison
Naval Research Laboratory
Code 6171
Washington, D.C. 20375-5000

Dr. C. A. Angell
Department of Chemistry
Purdue University
West Lafayette, Indiana 47907

Dr. D. F. Shriver
Department of Chemistry
Northwestern University
Evanston, Illinois 60201

Dr. Thomas Davis
Polymers Division
National Bureau of Standards
Gaithersburg, Maryland 20899

ABSTRACTS DISTRIBUTION LIST, 359/627

Dr. Stanislaw Szpak
Naval Ocean Systems Center
Code 633, Bayside
San Diego, California 95152

Dr. Gregory Farrington
Department of Materials Science
and Engineering
University of Pennsylvania
Philadelphia, Pennsylvania 19104

Dr. John Fontanella
Department of Physics
U.S. Naval Academy
Annapolis, Maryland 21402-5062

Dr. Micha Tomkiewicz
Department of Physics
Brooklyn College
Brooklyn, New York 11210

Dr. Lesser Blum
Department of Physics
University of Puerto Rico
Rio Piedras, Puerto Rico 00931

Dr. Joseph Gordon, II
IBM Corporation
5600 Cottle Road
San Jose, California 95193

Dr. Joel Harris
Department of Chemistry
University of Utah
Salt Lake City, Utah 84112

Dr. J. O. Thomas
University of Uppsala
Institute of Chemistry
Box 531 Baltimore, Maryland 21218
S-751 21 Uppsala, Sweden

Dr. John Owen
Department of Chemistry and
  Applied Chemistry
University of Salford
Salford M5 4WT UNITED KINGDOM

Dr. O. Stafsudd
Department of Electrical Engineering
University of California
Los Angeles, California 90024

Dr. Boone Owens
Department of Chemical Engineering
  and Materials Science
University of Minnesota
Minneapolis, Minnesota 55455

Dr. Johann A. Joebstl
USA Mobility Equipment R&D Command
DRDME-EC
Fort Belvoir, Virginia 22060

Dr. Albert R. Landgrebe
U.S. Department of Energy
M.S. 6B025 Forrestal Building
Washington, D.C. 20595

Dr. J. J. Brophy
Department of Physics
University of Utah
Salt Lake City, Utah 84112

Dr. Charles Martin
Department of Chemistry
Texas A&M University
College Station, Texas 77843

Dr. Milos Novotny
Department of Chemistry
Indiana University
Bloomington, Indiana 47405

Dr. Mark A. McHugh
Department of Chemical Engineering
The Johns Hopkins University
Baltimore, Maryland 21218

Dr. D. E. Irish
Department of Chemistry
University of Waterloo
Waterloo, Ontario, Canada
N21 3G1

ABSTRACTS DISTRIBUTION LIST, 359/627

Dr. Henry S. White
Department of Chemical Engineering
  and Materials Science
151 Amundson Hall
421 Washington Avenue, S.E.
Minneapolis, Minnesota 55455

Dr. Daniel A. Buttry
Department of Chemistry
University of Wyoming
Laramie, Wyoming 82071

Dr. W. R. Fawcett
Department of Chemistry
University of California
Davis, California 95616

Dr. Peter M. Blonsky
Eveready Battery Company, Inc.
25225 Detroit Road, P.O. Box 45035
Westlake, Ohio 44145

ABSTRACTS DISTRIBUTION LIST, 051A

Dr. M. A. El-Sayed
Department of Chemistry
University of California
Los Angeles, California 90024

Dr. E. R. Bernstein
Department of Chemistry
Colorado State University
Fort Collins, Colorado 80521

Dr. J. R. MacDonald
Chemistry Division
Naval Research Laboratory
Code 6110
Washington, D.C. 20375-5000

Dr. G. B. Schuster
Chemistry Department
University of Illinois
Urbana, Illinois 61801

Dr. J. B. Halpern
Department of Chemistry
Howard University
Washington, D.C. 20059

Dr. M. S. Wrighton
Department of Chemistry
Massachusetts Institute of Technology
Cambridge, Massachusetts 02139

Dr. W. E. Moerner
I.B.M. Corporation
Almaden Research Center
650 Harry Rd.
San Jose, California 95120-6099

Dr. A. B. P. Lever
Department of Chemistry
York University
Downsview, Ontario
CANADA M3J1P3

Dr. George E. Walrafen
Department of Chemistry
Howard University
Washington, D.C. 20059

Dr. Joe Brandelik
AFWAL/AADO-1
Wright Patterson AFB
Fairborn, Ohio 45433

Dr. Carmen Ortiz
Consejo Superior de
Investigaciones Cientificas
Serrano 121
Madrid 6, SPAIN

Dr. Kent R. Wilson
Chemistry Department
University of California
La Jolla, California 92093

Dr. G. A. Crosby
Chemistry Department
Washington State University
Pullman, Washington 99164

Dr. Theodore Pavlopoulos
NOSC
Code 521
San Diego, California 91232

Dr. John Cooper
Code 6173
Naval Research Laboratory
Washington, D.C. 20375-5000

Dr. Joseph H. Boyer
Department of Chemistry
University of New Orleans
New Orleans, Louisiana 70148

Dr. Harry D. Gafney
Department of Chemistry
Queens College of CUNY
Flushing, New York 11367-0904

Bis(Dioxolene)(Bipyridine)Ruthenium Redox Series

By A.B.P.Lever,* Pamela R. Auburn, Elaine S. Dodsworth, Masa-aki Haga[1a],
Wei Liu[1b], Milan Melnik[1c] and W. Andrew Nevin[1d]

Abstract

Complexes of the general formula $[Ru(bpy)(dioxolene)_2]^{n+}$ have been
prepared where (bpy) is 2,2'-bipyridine, and n = -1, 0, +1. The
dioxolene ligand is 1,2-dihydroxybenzene (catechol), 3,5-di-t-butyl- or
3,4,5,6-tetrachloro-1,2-dihydroxybenzene which may formally exist in the
catecholate, semiquinone or quinone oxidation state. Redox series of up
to five members have been prepared by controlled potential electrolysis
of the parent species or, in some cases, by chemical oxidation or
reduction. Electrochemistry, magnetism, X-ray structural data and
ultraviolet, visible and near infrared electronic, resonance Raman,
vibrational (FTIR), nuclear magnetic resonance, electron spin resonance
and photoelectron spectra, for various members of the redox series, are
discussed in terms of the electronic structures (effective oxidation
states, delocalization) of the complexes. Apparent conflicts between
results obtained using different techniques are resolved using a simple,
qualitative MO model.

Introduction

The concept of oxidation state is central to the understanding of inorganic chemistry. For covalently bonded substances, the oxidation state concept is a formalism based on conventions which enables the categorization of chemical behaviour and physical properties. These conventions break down in coordination complexes with extensive delocalization, such as the dithiolenes.[2] In such cases the oxidation state may no longer be defined as an integer, and the chemical properties are more easily explained using a molecular orbital model. Such delocalization was not thought to occur in dioxolene complexes,[3] but is shown to occur to a significant extent in the ruthenium complexes described here.

Metal complexes containing dioxolene ligands (di-oxo members of the catechol - quinone redox series) have been the subject of many recent publications.[3-11] The placing of two 'non-innocent' ligands on one central metal ion, which itself is redox-active, provides useful insight into metal-ligand bonding, intramolecular electron transfer and the concept of oxidation state in coordination chemistry.

We have recently reported electrochemical and spectroscopic data for a redox series based upon $Ru(bpy)_2(dioxolene)$ and $Ru(py)_4(dioxolene)$ where the dioxolene ligand was in the catechol, semiquinone or quinone oxidation state.[4] Electrochemical and spectroscopic data were presented to show that the ruthenium could be regarded as Ru(II) throughout this series, but that some delocalization occurred in the two oxidized species.[4,5] We describe here $Ru(bpy)(dioxolene)_2$ species where dioxolene is derived from 1,2-dihydroxybenzene (catechol, $CatH_2$), 3,5-di-t-butyl- ($DTBCatH_2$), or 3,4,5,6-tetrachloro-1,2-dihydroxybenzene ($TClCatH_2$).

The characterization of the oxidation states of the various

components (dioxolene ligands and metal) of these molecules presents difficulties; the electronic structures are not obvious from the molecular formulae. The two dioxolene ligands have a total of six accessible oxidation states, three for each ligand, and the ruthenium could be in the (II), (III) or (IV) oxidation state, giving nine possible combinations. Upon initial examination the various experimental techniques lead to conflicting conclusions, but it is shown that, by using a simple, qualitative MO model, the data can be rationalized in terms of fairly well defined but delocalized electronic structures.

Problems in assigning oxidation states have been encountered in Ru and Os ammines containing ligands with very low energy π^* orbitals which mix strongly with one of the metal d orbitals.[34,35] Some Os complexes, which formally contain metal(II), show charge transfer bands in their electronic spectra which behave like ligand to metal charge transfer (L--->Os(III)), and the $[Ru(II)(NH_3)_5(N\text{-methylpyrazinium})]^{3+}$ complex has a $Ru(3d_{5/2})$ photoelectron binding energy in the Ru(III) range.[36] The dioxolene data reported here provide additional insight into the electronic structures of such species.

Within a given redox series, the starting material as isolated from the initial synthesis is electrically neutral and is designated S. The symbols R1 and R2 refer to the first and second reduction products, and O1 and O2 to the first and second oxidation products, respectively.

For clarity, the abbreviation (diox) will be used for a general ligand without definition of its oxidation state. The labels (DTBCat), (DTBSq) and (DTBQ) etc. are used to indicate catecholate(-2), semiquinone(radical -1) and quinone(0) oxidation states where both substituent and oxidation state are defined. The labels cat, sq and q

are used for a species of defined oxidation state with indeterminate substituent. A label such as DTBDiox defines the substituent but not the oxidation state of the ligand.

Experimental

Methods: Electronic spectra were recorded with a Hitachi-Perkin Elmer microprocessor model 340 spectrometer or a Guided Wave Inc. model 100-20 Optical Waveguide Spectrum Analyser with a WP100 fiber optic probe. Electrochemical data were collected with a Pine model RDE3 double potentiostat or with a Princeton Applied Research (PARC) model 173 potentiostat or a PARC model 174A Polarographic Analyser coupled to a PARC model 175 Universal Programmer. Cyclic and differential pulse voltammetry were carried out using platinum wire working and counter electrodes, and a silver wire quasi-reference electrode. Potentials were referenced internally to the ferricenium/ ferrocene couple (Fc^+/Fc, 0.31 V vs SCE).[37] Spectroelectrochemical measurements utilized an optically transparent thin layer electrode (OTTLE) cell with a gold minigrid working electrode (500 lines/inch),[38] or a bulk electrolysis cell consisting of a platinum plate working electrode, and a platinum flag counter electrode and a silver wire quasi-reference electrode separated from the working compartment by medium glass frits. The fiber optic probe was immersed in the solution to obtain electronic spectra of the products.

Electron spin resonance spectra were obtained using a Varian E4 spectrometer calibrated with diphenylpicrylhydrazide. Where ESR spectra of electrochemically generated species were required, these were prepared under nitrogen inside a Vacuum Atmospheres Drilab and transferred to ESR tubes. Control electronic spectra were also recorded.

NMR data were obtained using a Bruker AM300 FT NMR spectrometer. Magnetic data were obtained through the courtesy of Prof. L.K. Thompson (Memorial University, Newfoundland) using a Faraday balance. Photoelectron spectra (PES) were recorded at the Surface Science Centre in the University of Western Ontario, London, Ontario. Fourier transform infrared (FTIR) data were obtained using a Nicolet SX20 spectrometer, as KBr disks or as Nujol or hexachlorobutadiene mulls. Resonance Raman (rR) data were obtained through the courtesy of Prof. D.J. Stufkens, University of Amsterdam, using apparatus and conditions as described previously.[39] Microanalyses were carried out by Canadian Microanalytical Service Ltd., New Westminster, BC.

Materials: Tetrabutylammonium perchlorate (TBAP, Kodak) was recrystallized from absolute ethanol and dried in a vacuum oven at 50°C for 2 days. 1,2-Dichlorobenzene (DCB, Aldrich Gold Label) and 1,2-dichloroethane (DCE, Aldrich Gold Label) were used as supplied. Dichloromethane and diethyl ether (Aldrich, Reagent Grade) were dried over molecular sieves and distilled under nitrogen prior to use. Ru(bpy)Cl$_3$ was prepared according to the literature.[40] Cobaltocene (Cp$_2$Co, Strem Chemical Company) was used as supplied. 3,5-Di-t-butylcatechol (Aldrich) was purified by recrystallization from benzene. Catechol was purchased from Tokyo Kasei or Aldrich, and was recrystallized twice from ethanol. 3,4,5,6-Tetrachlorocatechol was prepared by reduction of o-chloranil as follows. To a stirred solution of o-chloranil (2.0 g, 8.13 mmol) in glacial acetic acid (20 mL) was added dropwise a solution of SnCl$_2$·2H$_2$O (14 g; 62 mmol) in 12 M HCl (30 mL). The orange colour of the solution first darkened and then faded as the product precipitated. After complete addition, the resulting mixture was stirred at ambient temperature for 30 min. The crude product was

filtered, washed with 12 M HCl and then dried in vacuo. Recrystallization from EtOH/H_2O gave the monohydrate (88% yield). Mp 182-184°C, Lit[41] 194-195°C.

Preparation of Complexes: All manipulations were carried out under nitrogen or argon, with standard Schlenk techniques, except where stated.

Ru(bpy)(DTBDiox)$_2$ (1,S): To degassed methanol (30 mL) were added Ru(bpy)Cl$_2$ (0.29 g, 0.80 mmol) and DTBCatH$_2$ (0.34 g, 1.5 mmol). The resultant slurry was refluxed for 20 min. Addition of a solution of NaOH (0.12 g, 3.04 mmol) in methanol (10 mL) then gave a deep blue solution which was refluxed for 24 h. After cooling to room temperature the mixture was exposed to air, and water (5 mL) was added. Upon cooling (-5°C, 24 h) the product precipitated as a dark blue powder, which was recrystallized from methanol/water (87% yield). Samples for ESR were purified further by gel filtration on Sephadex LH20 using 1,2-dichloroethane as solvent. ^{1}H NMR data: (in C_6D_6 with 20% $CDCl_3$, scale ppm downfield from TMS) 7.64-6.40m; 1.68s; 1.67s; 1.34s; 1.33s; 1.31(4)s; 1.31(0)s; 1.26s. Anal. Calcd for $C_{38}H_{48}N_2O_4Ru$: C,65.4; H,6.9; N,4.0. Found: C,65.2; H,6.9; N,4.0.

Ru(bpy)(Diox)$_2$ (2,S): This compound was prepared using catechol in a procedure analogous to that described above for (1,S). After exposure of the reaction mixture to air, it was filtered immediately and allowed to stand at ambient temperature for 72 h. Deep blue crystals of the product were isolated by filtration and washed with methanol (45% yield). Samples for ESR were purified by gel filtration as above. ^{1}H NMR data: (in $CDCl_3$, scale ppm downfield from TMS) 8.31d (J = 8.03 Hz), 2H; 7.91td (J = 7.40, 1.66 Hz), 2H; 7.43 - 7.36m, 4H; 7.32dd (J = 8.16, 1.15 Hz), 2H; 7.16dd (J = 8.28, 1.35 Hz), 2H;6.94td (J = 7.14, 1.58 Hz), 2H;

6.84td (J = 8.24, 1.58 Hz), 2H. Anal. Calcd for $C_{22}H_{16}N_2O_4Ru$: C,55.8; H, 3.4; N, 5.9. Found: C,54.5; H.3.4; N,5.7. This compound was analysed several times and a better C analysis could not be obtained; it may be partially hydrated.

Ru(bpy)(TC1Diox)$_2$ (3,S): This compound was prepared - using tetrachlorocatechol in a procedure analogous to that described above for (1,S). After exposure to air the reaction mixture was left at ambient temperature for 48 h. Filtration of this mixture gave a crude material which contained primarily a dark green by-product. The desired product was extracted from this solid with several portions of boiling dichloromethane. The combined extracts were concentrated in vacuo and methanol was then added to initiate crystallization. This mixture was stored at -5°C for 72 h. Dark blue crystals of pure Ru(bpy)(TCIDiox)$_2$ (5% yield) were filtered off and washed with cold methanol. Anal. Calcd for $C_{22}H_8Cl_8N_2O_4Ru$: C,35.3; H,1.1; N,3.7. Found: C,34.8; H,1.1; N,3.4.

Ru(bpy)(DTBDiox)$_2$ClO$_4$ (1,01): To a stirred solution of Ru(bpy)(DTBDiox)$_2$ (69.9 mg, 0.098 mmol) in dichloromethane (3 mL) at 0°C, was added a solution of AgClO$_4$ (20 mg, 0.098 mmol) in acetonitrile (0.5 mL). Silver metal began to precipitate immediately and the mixture became deep purple. After 15 min the mixture was filtered through a short plug of celite (7 mm x 50 mm) to remove the metallic silver. The volume of the filtrate was reduced to 2 mL and a mixture of diethyl ether and hexanes was added to initiate crystallization. The mixture was left at -5°C for 24 h. After filtration, purple crystals of the product were obtained (91% yield). Anal. Calcd for $C_{38}H_{48}ClN_2O_8Ru$: C,57.2; H,6.1; N,3.5. Found: C,56.8; H,6.1; N,3.7. The hexafluorophosphate salt was prepared similarly, using AgPF$_6$ in place of AgClO$_4$; its spectra (IR and electronic) were in agreement with those of the perchlorate.

[Cp₂Co][Ru(bpy)(Diox)₂] (**2,R1**): Cobaltocene (50.2 mg, 0.27 mmol) was added to a solution of Ru(bpy)(Diox)₂ (0.112 g, 0.24 mmol) in dichloromethane (30 mL) in an oxygen-free environment (dry box). The resulting dark green solution was stirred for 2 h and then filtered under pressure in the dry box. The dark green microcrystalline product (84% yield) was washed with diethyl ether and dried in vacuo. Anal. Calcd for $C_{32}H_{26}CoN_2O_4Ru$: C,58.0; H,4.0; N,4.2. Found: C,54.8; H,3.9; N,4.1. Some difficulty was experienced in obtaining a better C analysis for this product; its electronic spectrum is in agreement with the spectroelectrochemical data.

Results

Two series of compounds were prepared; one is based on Ru(bpy)(diox)₂, necessarily with a cis configuration, and the other is a series of cis- and trans-Ru(R-py)₂(diox)₂, to be described elsewhere,[42] but whose comparative electronic properties are relevant to the discussion of the bpy series. The materials obtained from the reaction mixture, Ru(bpy)(diox)₂, the so-called starting materials, (labelled **S**) possess no counter ions, and are air-stable, dark blue crystalline compounds. Single crystal X-ray data are available for the Ru(bpy)(Diox)₂ (**2,S**) species (Figure 1),[43] and for the related trans-Ru(4-t-Bupy)₂(DTBDiox)₂, (**4t,S**) compound.[44,45] Relevant bond distances are shown in Table I. One example each of an oxidized and reduced complex was isolated in the solid state.

i) Electrochemistry: Table II contains electrochemical data for the starting materials, generally showing five one-electron redox processes (Fig.2), near +1.4-1.5 (I), +0.9-1.2 (II), +0.2-0.9 (III), 0-(-0.8) (IV)

and −0.9−(−1.5) (V) V vs SCE. The bulk solution rest potentials for the starting materials lie between redox couples (III) and (IV). Couples (II)−(V) are usually reversible (but see Table II for details) showing $i_c/i_a = 1$, $i \propto \sqrt{v}$ and peak to peak separations in the cyclic voltammogram (for reversible species) approaching 60 mV at slow scan rates (20 mV s^{-1}). The oxidation process (I) is invariably irreversible. The oxidized species [Ru(bpy)(DTBDiox)$_2$]ClO$_4$ (**2,01**), in bulk solution, gives similar voltammetry (the same redox couple potentials) to the starting material in DCE, but has a different rest potential. The reversibility of most of the couples is an indication that structural changes such as dimerization or ligand loss are not taking place on the time scale of the experiment.

ii) **Nuclear magnetic resonance spectra:** The starting materials all give sharp and unshifted NMR spectra, implying the absence of paramagnetic species in the solutions.[44-46] For the (necessarily cis) Ru(bpy)(DTBDiox)$_2$ (**1,5**) there are three possible structural isomers depending upon the relative positions of the t-butyl groups on the two dioxolene ligands. These three isomers give rise to eight possible t-butyl resonances. In fact seven may be observed using a 20% CDCl$_3$ in C$_6$D$_6$ solvent mixture, showing that all three isomers are present in solution, and that there is an accidental degeneracy of two resonances.

iii) **Magnetic susceptibility measurements:** The d^5 species [Ru(bpy)(DTBDiox)$_2$]ClO$_4$ (**1,01**) has one unpaired electron/molecule and a Curie-Weiss dependence of the magnetic susceptibility (χ_M = 0.329/(T + 4.78), R = 0.999, 32 points). The room temperature (295 K) moment is 1.63 BM, declining gradually to 1.51 BM at 5 K.

Although their solutions appear diamagnetic from the NMR data, the solid starting materials, S, have moments of the order of 1 BM/molecule or less at room temperature, consistent with temperature independent paramagnetism.

iv) **Electron spin resonance spectra:** The starting materials, (**1,**S) and (**2,**S), are ESR-silent at room temperature (solid or solution) and at 77 K in frozen DCE. In the solid state at 77 K very weak signals can be detected at $g = 2$; these are believed to be due to trace amounts of a free radical impurity since stronger signals are observed in samples which have not been purified by gel filtration. The R1 and O1 species yield rather broad signals very close to $g = 2$ in solution at room temperature, but at 77 K in the solid state, or in frozen DCB solution, sharp, free radical-like, axial or slightly rhombic signals are observed (Fig.3, Table III). For the oxidized species, O1, $g_{\parallel} > g_{\perp}$, while the reverse is true for the reduced species; the difference between $g_{\parallel}$ and $g_{\perp}$ is ~0.2 for R1 and ~0.04 for O1.

The electrochemically generated R2 species are ESR-silent at room temperature and at 77 K. Solutions of O2 are unstable.

v) **Fourier transform infrared spectra:** The principal FTIR absorption bands are given in Table IV. None of the starting materials show features typical of either catechol or semiquinone coordination. The spectra of all the S species (including the cis- and trans-R-py analogues)[42] are dominated by a strong absorption in the region 1100 - 1200 cm^{-1} (Figure 4). The FTIR spectrum of a reduced complex (Figure 4) is consistent with the presence of a catecholate moiety, but that of an oxidized species (Fig.4) does not provide clear evidence of oxidation

state.

vi) **Photoelectron spectra:** Data for the $Ru(3d_{5/2})$ and core levels of oxygen and nitrogen are shown in Table V. The lowest $Ru(3d_{5/2})$ binding energy occurs in R1 and the highest in O1. The N(1s) and O(1s) energies follow roughly the same trend, but with smaller differences.

vii) **Electronic spectra:** Table VI contains electronic spectroscopic data for the starting materials and a selection of their oxidation and reduction products. Clean reactions with isosbestic points were generally observed in these redox processes. The electronic spectra of O2, O1, S, R1 and R2 are shown for the (**1**) redox series in Figure 5. In general, all members of a given oxidation label, i.e. O1, R1, etc., have very similar shaped spectra. Many of the absorption bands show significant dependence upon the dioxolene substituent. Spectra of representative complexes in the solid state (in nujol mulls) are similar to the corresponding solution spectra. The S series is remarkable in the very intense near IR absorption, absent from all other oxidation states, but present in the mono-semiquinone ruthenium species.[4] Resonance Raman spectra of three compounds were obtained in order to clarify the assignments of the spectra (see Table VII). Full details of these will appear elsewhere.[47]

Discussion

In the previous dioxolene literature, mixed valence compounds have generally been interpreted in terms of localized structures.[11,16,44] Moreover, in Co(bpy)(DTBSq)(DTBCat) and Mn(py)$_2$(DTBSq)$_2$ discontinuous changes in formal oxidation state have been observed with change of

temperature.[13,23,44] Nevertheless, ESR studies of many dioxolene complexes have shown that delocalization occurs to a small extent,[6,9,48] and in one recent case this has been supported by extended Hückel and fragment molecular orbital calculations.[48] However, it has been thought previously that extensive delocalization did not occur in dioxolene complexes, and that oxidation states could be unambiguously defined.[3] Ruthenium dioxolenes are the first dioxolene complexes in which significant delocalization has been demonstrated.[4,5]

Using the normal oxidation state conventions, with localization of electrons, these species could exist as a number of possible electronic isomers. The following are the most reasonable possibilities:

R2　　a)　　$[Ru(II)(bpy)(cat)_2]^{2-}$

　　　　b)　　$[Ru(III)(bpy^-)(cat)_2]^{2-}$

R1　　a)　　$[Ru(II)(bpy)(cat)(sq)]^-$

　　　　b)　　$[Ru(III)(bpy)(cat)_2]^-$

S　　　a)　　$Ru(II)(bpy)(sq)_2$

　　　　b)　　$Ru(III)(bpy)(cat)(sq)$

　　　　c)　　$Ru(IV)(bpy)(cat)_2$

O1　　a)　　$[Ru(II)(bpy)(sq)(q)]^+$

　　　　b)　　$[Ru(III)(bpy)(sq)_2]^+$

　　　　c)　　$[Ru(IV)(bpy)(cat)(sq)]^+$

O2　　a)　　$[Ru(II)(bpy)(q)_2]^{2+}$

　　　　b)　　$[Ru(III)(bpy)(sq)(q)]^{2+}$

c) $[Ru(IV)(bpy)(sq)_2]^{2+}$
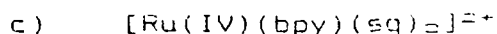
We consider first the oxidation state information which may be derived from the various techniques.

All the redox potentials depend significantly upon the substituents in the dioxolene ring. Upon replacement of DTBCat by TClCat the potentials shift 0.36, 0.68, 0.82 and 0.58 V for couples (II) through (V) respectively. Similar dependencies are seen in the corresponding trans-4-t-butylpyridine data set,[42] except for couple (V) whose dependence essentially disappears. A large dependence may imply a redox process which is localized on the dioxolene ligands, while a small or zero dependence indicates a redox process on the metal ion.[49] In the $Ru(bpy)_2(diox)$ and $Ru(py)_4(diox)$ series, the shifts in both redox processes involving the dioxolene ligands were about 0.5 V when TClDiox replaced DTBDiox.[4] Differences of about 0.7 V are observed for both the free ligands reductions (q/sq and sq/cat) when comparing TClDiox and DTBDiox,[8] and larger differences (0.7 – 1.2 V) occur in the complexes[11] $Cr(III)(bpy)(sq)(cat)$ and[9] $[Cr(III)(cat)_2]^{2-}$.

With regard to ESR spectra, we are concerned with distinguishing a Ru(III) centre from a Ru(II) centre bound to a free radical. Low spin Ru(III) $(t_{2g})^5$ species exhibit ESR spectra which are usually highly anisotropic with axial or rhombic symmetry.[50] For example, $[Ru(III)(NH_3)_4(cat)]^+$ cations give axial spectra with $g_{\parallel}$ = ~1.9 and $g_{\perp}$ = ~2.7.[46] On the other hand a radical bound to Ru(II) will exhibit a narrow signal close to g = 2. Nevertheless, in certain reduced $[Ru(bpy)_3]^{(2-n)+}$ species, ligand-localized electrons show slightly anisotropic signals with $g_{\parallel} < g_{\perp}$ and differences of up to ~0.04 between the g values.[51] Ruthenium phosphine semiquinone complexes,[52,53] also

with $g_{\parallel} < g_{\perp}$, have similar anisotropy ($g_{\parallel} = 2.00$, $g_{\perp} = 2.02$). The [Ru(bpy)$_2$(DTBSq)]$^+$ cation[4] shows slight anisotropy, $g_{\parallel} > g_{\perp}$, similar to the O1 species.

The IR spectra of dioxolene complexes can normally be used without ambiguity to define the oxidation state of the dioxolene ligand.[19,46,54-56] The C-O frequency is particularly characteristic and gives rise to relatively intense absorption at:[16-19,46,54-57]

Coordinated quinones	C=O	1600-1675 cm^{-1}
semiquinones	C-O	1400-1500
catechols	C-O	1250, 1480 (ring breathing)

The strong band observed near 1150 cm^{-1} in the S series complexes has almost no precedent in the literature. Strong bands in this region have been reported in only one other case, a series of 4-coordinate copper(II) complexes of DTBSq with nitrogen-donor co-ligands.[32] These complexes show one or two strong bands between 1110 and 1160 cm^{-1}, which were not assigned, and there are no strong features in the 1450 cm^{-1} region where typical semiquinone absorptions occur.

Using PES, inner shell binding energies of metals in complexes may be used (with caution) to infer the oxidation state of the metal.[58a] Typically, the binding energy increases by about 1 eV per unit increase in oxidation state regardless of the charge on the metal.[58b] There are exceptions, however, particularly where π-bonding ligands are present. Comparisons are best made within a series of complexes having similar ligands. The $3d_{5/2}$ binding energies for Ru(II) and Ru(III) normally lie in the ranges 280-282 and 282-283 eV respectively,[54,58] though a binuclear species formally containing both Ru(III) and Ru(IV) shows only one peak at 282.9 eV,[58a] and an (N-methylpyrazinium)ruthenium pentaammine complex which formally contains Ru(II) has a binding energy

of 292.2 eV, in the Ru(III) range.[58] The nitrogen 1s binding energy is known to be sensitive[59] to variation in charge on the atom to which it is bound. However, the variation in N(1s) energies in this series of complexes is too small to draw any conclusions.

Following the discussion of electronic spectra presented previously,[4] one may observe metal to ligand charge transfer (MLCT) from Ru($d\pi$) to acceptor orbitals on bpy, sq or q, and/or ligand to metal charge transfer (LMCT) from cat, sq, or bpy to Ru(III), internal semiquinone, and interligand charge transfer (ILCT) transitions, all of which might occur in the visible region. The charge transfer transitions will have energies depending on the oxidation state of ruthenium and the dioxolene ligand, and should depend in a predictable manner on the dioxolene substituents. The weaker ligand field transitions are likely to be obscured in these systems.

Catecholate derivatives of difficult to reduce metal ions show no visible absorption other than d-d;[28,53,60,61] e.g.[M(II)(cat)$_2$]$^{2-}$ (M=Co,Ni,Cu). However, catecholate complexes of a reducible metal should show LMCT transitions. For example, complexes of iron(III), cerium(IV) and higher oxidation states of molybdenum and manganese show moderately intense (2000-5000 L mol^{-1} cm^{-1}) visible region transitions attributable to LMCT.[21,-5,61-67] These might also be observed, shifted to the blue, in a semiquinone bound to a reducible metal ion.

The internal transition observed in the visible region in free semiquinones may also be observed as a weak absorption (ϵ ca. 800 - 5000 L mol^{-1} cm^{-1}) in semiquinone metal complexes, shifted a little from its free ligand position; e.g. DTBSq$^-$ 690 nm (800), Zn(II)(DTBSq)$^+$ 740 nm (900),[19] [Co(trien)(DTBSq)]$^{2+}$ 512 nm (1200)[68], and M(II)(DTBSq)$_2$(bpy) (M=Mn,Co,Ni) ca. 770 nm (2700).[13,14] A band similar in energy and

intensity (ca. 700 nm (2500)) is seen[11] in [Cr(III)(DTBSq)$_2$(bpy)]$^+$, but in this case there is also a more intense transition near 500 nm (7400). A similar transition (similar band envelope), with a molar absorption coefficient of almost 20,000 L mol^{-1} cm^{-1}, is observed in Cr(III)(DTBSq)$_3$.[11,14] It is unlikely that Cr(III) would exhibit such a low energy LMCT transition, particularly as there is no such band in[14] [Cr(DTBCat)$_3$]$^{3-}$, so this transition probably also involves only the semiquinone ligands.

Complexes containing both a sq and a cat residue sometimes exhibit a broad, relatively weak (ca. 3000 L mol^{-1} cm^{-1}) transition in the red or near infrared (NIR) region which has been attributed to an intervalence (interligand) transition.[16,44]

Five orbital model:

The electronic structure, spectra, magnetism and ESR of these species can be understood by using a simple, qualitative MO model constructed from the three 4d (t_{2g} in O_h) ruthenium orbitals and the frontier π ($3b_1$ in C_{2v} using the Gordon and Fenske nomenclature[69]) orbitals of the dioxolene ligands. We refer to this below as the five orbital model. From electrochemical data, it is evident that the bipyridine LUMO π_1^* is sufficiently high in energy,[70] and the dioxolene oxygen lone pairs ($a_1 + b_2$, in dioxolene plane) are sufficiently low (and have little overlap), that they are not considered to play a major role in influencing the oxidation states of metal and ligands. They are, however, relevant to the electronic spectra.

In the (maximum) C_2 symmetry of these species, the two ligand $\pi(3b_1)$ orbitals combine to yield (a + b) and the three d orbitals transform as (a + 2b). One ligand combination will couple to two d

orbitals, and the other to only one, resulting in a pronounced splitting of these ligand combinations. The three d orbitals all possess some ligand character (and vice versa) depending upon orbital overlap and the relative d and L orbital energies. These five MOs are filled with ten electrons in R2.

All five orbitals will become more stable going from R2 to O2, but those which are primarily metal in character will be stabilized more upon oxidation of the complex than those which are primarily ligand,[4,69,70] because of the greater spatial extent of the ligand orbitals. From the data discussed below, oxidation of R2 involves oxidation of Ru(II), at least to some degree; thus the ruthenium d(a,2b) orbitals lie at comparable or slightly higher energies than the catechol (a,b) combinations in R2. To be consistent with all the experimental data, proceeding from R2 to O2 there must then be a crossover of these orbitals such that at O2 the ruthenium d(a,2b) orbitals lie below the ligand combinations (see Figure 6).

In the crossover region there will be extensive mixing of the d(a,2b) and L(a,b) orbitals. Placing 9, 8 and 7 electrons into these five mixed orbitals, from R1 to O1, yields, from experiment, 1, 0 and 1 unpaired electrons respectively, and leaves the uppermost level of the five half-full in R1 and empty in S and O1. This approach is validated in the trans-Ru(R-py)$_2$(diox)$_2$ series[42] where two of the three d orbitals are unmixed because of the higher symmetry (D_{2h}). It is evident that one of these d orbitals is uppermost in the [Ru(3-Clpy)$_2$(DTBCat)$_2$]$^-$ R1 species which is exclusively Ru(III), as indicated by its typical rhombic ESR spectrum.[42]

The effective oxidation state of the metal is determined by the total number of electrons in each MO scaled by the d orbital

contribution to that MO. Similarly the average effective oxidation state of the pair of dioxolene ligands is determined by the total scaled occupancy of all orbitals having a contribution from the dioxolene ligands. Since the uppermost (of the five) orbital in R1 contains one unpaired electron, and this orbital is mixed Ru(d) and L, then an electron count must lead to the conclusion that the central ion in R1 is between Ru(II) and Ru(III), shifting to the latter as this orbital approaches a pure Ru(d) orbital. Similar arguments can be applied to the other members of the redox series. On passing from R1 to O2 the upper orbitals will contain an increasing proportion of L(a,b) so that the more oxidized species will approximate more closely to ruthenium(II).

Using the five orbital model, the structural and electronic identification of the various members of the redox series can be approached. Since this qualitative model does not indicate the ordering within the group of metal or ligand orbitals per se, for the purpose of assigning electronic transitions the general labels, $Ru(d\pi)$ and $diox(3b_1)$, are used to designate orbitals of mainly metal and mainly dioxolene ($3b_1$) origin respectively (see Table VIII and discussion below).

Electronic structural assignments:

Species R2: These highly air-sensitive compounds were not isolated from solution; they are characterized by their electronic spectra and redox potentials. Referring to the possible electronic structures described above, reduction of the bipyridine ligand (R2,b) can be eliminated with three arguments, a) the potential (V) is insufficiently negative,[70] b) the pyridine series[71] have the R1/R2 couple in the same region, c) there

are no low lying absorption bands typical of a bpy⁻ ion.[21] Thus R2 complexes are regarded as [Ru(II)(bpy)(cat)$_2$]$^{2-}$.

There should be no low energy charge transfer between metal and catechol. A low energy Ru(dπ)--->bpy($π_1$*) is expected, and possibly a low energy ILCT transition from catecholate ($3b_1$)--->bpy($π_1$*). The overall band envelope looks very similar to that in Ru(II)(bpy)$_2$(DTBCat) (**5,R1**),[4] and the broad absorption at 700-900nm is similarly assigned to both Ru(dπ)--->bpy($π_1$*) and cat($3b_1$)--->bpy($π_1$*). The bpy complex shows a band near 500 nm which is absent from the trans-R-py series and may contain Ru(dπ)--->bpy($π_2$*). Both these Ru(dπ)--->bpy($π$*) MLCT transitions lie lower in energy than in (**5,R1**) as expected on replacement of a bpy by DTBCat.

<u>Species R1</u>: The uppermost of the five orbitals discussed above will contain one unpaired electron. Visible region electronic transitions, other than those to bipyridine, will probably terminate on this orbital. Since these transitions shift to the blue with increasing acceptor character of the dioxolene ligand (Table VI), i.e. behave as LMCT transitions,[22] the inference is that the uppermost orbital has significant d character. On this evidence, R1 must have a major contribution from [Ru(III)(bpy)(cat)$_2$]$^-$.

The Ru($3d_{5/2}$) PES core energy (Table V) appears consistent with the presence of Ru(II). However, the PES data do not exclude Ru(III) since the trans-[Ru(3-Clpy)$_2$(DTBCat)$_2$]$^-$ R1 species, which, from ESR evidence, undoubtedly contains Ru(III), has a binding energy of 281.4 eV,[22] within the Ru(II) range, the core energy probably being depressed because of the inductive effect of the DTBCat ligands. The ESR spectra of (**1,R1**) and (**2,R1**) (Table III) give g values very close to the free radical value of 2, but their axial symmetry at low temperature suggests a

significant contribution from Ru(III). The FTIR data are inconclusive, showing a typical catechol ν(C-O) around 1250 cm^{-1}, and a strong band at 1415 cm^{-1} (Table IV) which could be either the expected catechol ring stretching mode, occurring at a similar frequency to that in the Ru(bpy)$_2$(cat) series, or the ν(C-O) of a coordinated semiquinone. The latter could only occur in a localized (Class I,II) mixed valence system, [Ru(II)(bpy)(sq)(cat)]$^-$, since in a delocalized (class IIIa) system an average of sq and cat ν(C-O) frequencies would be expected. Localized configurations are excluded by the five orbital model.

Finally, the substituent dependence of the R1/R2 couple (V) (Table II) is too small to be associated with a purely sq/cat redox process, and too large for a Ru(III)/Ru(II) couple. Thus this redox process probably involves both metal and ligand.

The electronic spectrum of R1 is most easily interpreted on the basis of the formula [Ru(III)(bpy)(cat)$_2$]$^-$. The strong band at around 700 nm is assigned primarily as cat(3b$_1$)--->Ru(III)(t$_{2g}$^{5}) LMCT. A CT band, which can only be cat--->Ru(III), is observed in a similar position in [Ru(III)(NH$_3$)$_5$(Cat)]$^+$.[46] The broad, lower energy band is probably cat(3b$_1$)--->bpy(π_1^*); this is also expected to blue shift as the catechol becomes a better electron acceptor. If the R1 species were deemed to exist purely in the [Ru(II)(bpy)(sq)(cat)]$^-$ form, then an intense Ru(dπ)--->sq(3b$_1$) transition, analogous to those in S and [Ru(bpy)$_2$(sq)]$^+$, would be expected to occur in the NIR below 950 nm; such a transition is not observed.

Thus the data can be explained in terms of an effective ruthenium oxidation state between Ru(II) and Ru(III), but closer to Ru(III). In valence bond terminology R1 is predominantly [Ru(III)(bpy)(cat)$_2$]$^-$ but with a resonance contribution from [Ru(II)(bpy)(cat)(sq)]$^-$.

Species S: Since these species are diamagnetic, the separation of the ligand a and b combinations must be great enough to cause spin pairing in the lower energy combination. The uppermost level is now empty (LUMO) and the five orbital model predicts that it has more ligand character (Figure 6) than in R1, and therefore that the species should be closer to Ru(II) in character. The X-ray structure of (2,S)[43] shows equivalent C-O distances (Table I) intermediate between those expected for sq and cat ligands.[19] Moreover the small thermal ellipsoids, elongated away from the C-O bond axes, indicate that the X-ray structure is not disordered. Evidently the dioxolene ligands are equivalent and intermediate between the catecholate and semiquinone forms. The PES data (Table V) for (1,S) and (2,S) are indicative of Ru(II), though (2,S) has a higher binding energy, probably reflecting the less basic dioxolene ligands.

The FTIR spectra (Table IV) are difficult to interpret. As the bond lengths in (2,S) are midway between those of catechol and semiquinone the C-O stretch would be expected (naively) to lie between 1250 and 1450 cm^{-1}. Species (2,S) shows a strong band in this region, at 1414 cm^{-1}, but the other complexes do not. The strongest bands in the spectra (1100-1200 cm^{-1} region) are too low in frequency for a simple assignment as ν(C-O), since this would imply (taking a simplified view) a C-O bond weaker than the single C-O bond of a coordinated catechol. However, the recent observation of similar bands in copper(II) semiquinone complexes[22] suggests that at least one ligand approximates to a semiquinone. The unusual FTIR spectra probably result from the low symmetry of these molecules and the extensive coupling expected between the various vibrational modes of the ligands,[23] and between the three ligands via the ruthenium.

The electronic spectra are typified by a strong band in the NIR (see Figure 5), with a well defined lower energy shoulder or peak. Both the high intensity and narrow width of the NIR band are inconsistent with this absorption being due to intervalence (cat--->sq) transitions.[16,44] The peak is very similar to NIR absorption in the spectrum of $[Ru(II)(bpy)_2(DTBSq)]^+$ (**5,S**),[4] and is similarly assigned to $Ru(d\pi)$---->$sq(3b_1)$. Accordingly, there is a small red shift upon replacement of DTBSq by TClSq (Table VI). In the C_2 symmetry, transitions to L(a,b) from all three d orbitals are allowed, and therefore the two components of the NIR band probably reflect the d orbital splitting.

In the visible region there is a strong band near 600nm and a weaker shoulder or peak near 500nm. Ru(II)-bpy complexes show a $Ru(d\pi)$--->$bpy(\pi_1^*)$ transition with a molar absorption coefficient of approximately 4000 L mol^{-1} cm^{-1} per bpy ligand,[72] thus the 600 nm band is too strong to be so assigned, whereas the weaker band has approximately the expected intensity. In the rR spectrum of (**1,S**) bpy vibrations are enhanced when irradiating into the weaker band near 500 nm (and similarly for the 450 nm band of (**3,S**)) (Table VII). The frequencies agree well with the rR spectrum of the $[Ru(bpy)_3]^{2+}$ cation.[74] The weaker visible region band is then identified as $Ru(d\pi)$--->$bpy(\pi_1^*)$, an assignment supported by its appearance at roughly the expected energy, calculated by extrapolating from $[Ru(bpy)_3]^{2+}$ and $[Ru(bpy)_2(DTBSq)]^+$. This transition shifts to the blue when DTBCat is replaced by TClCat, consistent with some stabilisation of the ruthenium d orbitals.

There remains the assignment of the strong 600 nm band. The rR data for irradiation at 570 nm show significant enhancement of vibrations

which can be assigned to Ru-O stretching modes and deformation modes of the dioxolene ligand.[47] Thus the 600 nm band is associated with the dioxolene rather than the bipyridine ligand. This conclusion also follows from the presence of a similar band in the spectra of the cis-$(R-py)_2Ru(diox)_2$ S species.[42] Two possible assignments can be considered. The first is a second MLCT transition similar to the NIR band (since the intensities are comparable) arising from a large splitting of the d ("t_{2g}") orbitals. Such a splitting (~ 6000 cm^{-1}) is unlikely as there is no bonding mechanism to discriminate between the three d orbitals to such an extent.

Alternatively, the transition may be related to the internal semiquinone, $n \rightarrow \pi^*$, transition which occurs in this region in the free ligand.[10] The oxygen lone pair orbital combinations span (2a + 2b) and may therefore mix with the ruthenium d orbitals; the relatively high intensity of this transition and the rR data require that the $n \rightarrow \pi^*$ transition have some $\pi \rightarrow \pi^*$ Ru-O character. This assignment is supported by the small blue shift that occurs on replacement of DTBDiox by TClDiox, consistent with some LMCT character. The transition is effectively from the lone pair of one semiquinone to the π^* of the other, the latter being strongly mixed with the metal orbitals. This transition is never observed as a prominent feature in the spectra of mono-semiquinone metal complexes[4,22] or in the trans-$(R-py)_2Ru(diox)_2$ S species[42] because the forbidden character (no overlap to first order) of the $n \rightarrow \pi^*$ cannot be overcome in D_{2h} symmetry. In cis-bis-semiquinone species, this transition is strong only when there is significant metal-semiquinone mixing, for example in Cr(III) complexes.[11,14] In the absence of such mixing (e.g. in complexes of Mn, Fe, Co and Ni[15,16,44]), the transition remains fairly localized and hence weak.

The S species are therefore best regarded as Ru(II)(bpy)(sq)$_2$, with significant mixing of metal and ligand orbitals, through Ru-sq π back-bonding, causing elongation of the C-O bonds. The R1 to S oxidation involves conversion of two mainly catecholate ligands to two mainly semiquinone ligands; the large shift in the potential of this couple upon replacement of DTBCat by TClCat is consistent with this conclusion.

Species O1: The upper two orbitals should now be mainly ligand in character, and contain one electron. Thus the effective oxidation state lies between Ru(II) and Ru(III), but much closer to the former. The formulation [Ru(II)(bpy)(sq)(q)]$^+$ must, in this model, have equivalent (delocalized) dioxolene ligands, i.e. a class III mixed valence species.[25]

The PES Ru(3d$_{5/2}$) binding energy lies on the boundary between "normal" Ru(II) and Ru(III) (Table V). The FTIR data (Table IV, Figure 4) do not show clearly the presence of either quinone or semiquinone. The magnetic data and ESR spectrum (Table III) indicate the presence of only one unpaired electron and exclude an uncoupled [Ru(III)(bpy)(sq)$_2$]$^+$ formulation. The ESR spectrum is consistent with a free radical, but with a very small g anisotropy which is the opposite of that typically observed for axial Ru(III)[30] and also for reduced bpy in [Ru(bpy)$_3$]$^{(2-n)+}$,[31] but the same as in [Ru(bpy)$_2$(DTBSq)]$^+$.[4] The proportion of Ru(III) in O1 is predicted, by the five orbital model, to be less than in R1, and this is confirmed by the ESR data where the g anisotropy is considerably smaller in O1 than in R1.

The electronic spectra (Table VI) show two intense bands in the visible region, near 720 and 545 nm. Both shift to the red as the ligand becomes more electron withdrawing, consistent with MLCT, confirming that the LUMO is now mainly ligand in character. These two bands are

comparable in intensity and in energy separation with the strong NIR and visible region bands in the S complexes, which suggests that they may have similar assignments. As in the S series, the higher energy band is present only very weakly (at 520-580 nm) in the trans-pyridine O1 series, but more strongly in the cis-pyridine series.[42] This evidence supports the formulation [Ru(II)(bpy)(sq)(q)]$^+$.

RR spectra (Table VII) in the visible region show enhancement of mainly low energy modes, corresponding to dioxolene deformations and ν(Ru-O).[47] Data have not been obtained for direct excitation into the 720 nm band, but it appears (from excitation at 620 nm into the tail of this band) that the same frequencies are enhanced in both transitions. This precludes assignment of the transitions as localized Ru(dπ)--->q(3b$_1$) and Ru(dπ)--->sq(3b$_1$), but it is consistent with assignments similar to those given above for S (see Table VIII). An additional transition is also expected from Ru(dπ) to the partly occupied lower ligand combination orbital. This may account for the absorption between the two peaks in the visible region. The band at 400 nm almost certainly involves Ru(dπ)--->bpy(π_1*), shifted to higher energy from the S species due to stabilization of the Ru d orbitals.

Species O2: The trends discussed above and the five orbital model predict that O2 will be [Ru(II)(bpy)(q)$_2$]$^{2+}$, but there are insufficient data available to confirm this.

Summary and Conclusions

The electronic structures of the various species may be represented as:

R2   [Ru(II)(bpy)(cat)$_2$]$^{2-}$

R1 $[Ru(III)(bpy)(cat)_2]^-$ <--> $[Ru(II)(bpy)(cat)(sq)]^-$

S $Ru(II)(bpy)(sq)_2$ <--> $Ru(III)(bpy)(cat)(sq)$

O1 $[Ru(II)(bpy)(sq)(q)]^-$ <--> $[Ru(III)(bpy)(sq)_2]^+$

O2 $[Ru(II)(bpy)(q)_2]^{2+}$
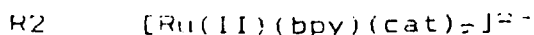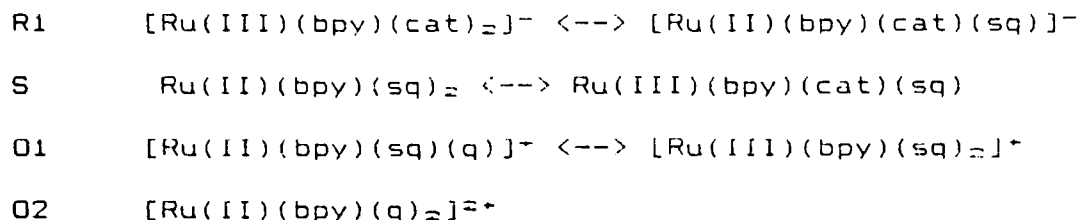
with the first cited species being dominant, and with extensive overlap between the ruthenium d orbitals and dioxolene frontier orbitals, i.e. extensively delocalized. There has been no substantial evidence previously for delocalization to this extent in dioxolene complexes;[3] these data therefore represent the first such detailed evidence for this behaviour.

The various techniques undertaken here all provide a measure of the effective oxidation state but there are frequently ambiguities in interpretation. PES in particular was not as useful as we had hoped since it measures the net charge felt by inner electrons, which in these complexes strongly reflects the basicity of the ligands. For localized systems FTIR usually provides a useful guide to the oxidation state of the dioxolene ligand. In delocalized mixed-valence systems it is potentially useful but requires full analysis of the spectra. ESR and electronic spectra, especially when supported by resonance Raman spectroscopy, provide the most accurate representations. A more detailed MO analysis of the various members of these redox series is in hand and should give further clarification.

for advance information on the crystal structure of Ru(bpy)(Diox)$_2$, and
Professors L.K. Thompson and D.J. Stufkens for the magnetism and
resonance Raman measurements respectively.

References

1. Current addresses a) Dept. of Chemistry, Mie University, Japan.
   b) Dept. of Chemistry, Yangzhou Teacher's College, Jiangsu, People's
   Republic of China. c) Dept. of Chemistry, Slovak Technical
   Institute, Bratislava, Czechoslovakia. d) Central Research
   Laboratories, Kanegafuchi Chemical Industry Co. Ltd., Kobe 652,
   Japan.

2. (a) McCleverty, J. A. Progr.Inorg.Chem. 1968, 10, 49.
   (b) Schrauzer, G. N. Accts.Chem.Res. 1969, 2, 72.

3. Pierpont, C. G.; Buchanan, R. M. Coord.Chem.Rev. 1981, 38, 45.

4. Haga, M.; Dodsworth, E. S.; Lever, A. B. P. Inorg.Chem. 1986, 25,
   447.

5. Boone, S. R.; Pierpont, C. G. Inorg.Chem. 1987, 26, 1769.

6. Cass, M. E.; Gordon, N. R.; Pierpont, C. G. Inorg.Chem. 1986, 25,
   3962.

7. Lynch, M. W.; Buchanan, R. M.; Pierpont, C. G.; Hendrickson, D. N.
   Inorg.Chem. 1981, 20, 1038.

8. Stallings, M. D.; Morrison, M. M.; Sawyer, D. T. Inorg.Chem. 1981,
   20, 2655.

9. Downs, H. H.; Buchanan, R. M.; Pierpont, C. G. Inorg.Chem. 1979,
   18, 1736.

10. Bodini, M. E.; Copia, G.; Robinson, R.; Sawyer, D. T. Inorg.Chem.
    1983, 22, 126.

11. Buchanan, R. M.; Claflin, J.; Pierpont, C. G. Inorg.Chem. 1983, 22,
    2552.

12. Kahn, O.; Prins, R.; Reedijk, J.; Thompson, J. S. Inorg.Chem. 1987,
    26, 3557.

13. Lynch, M. W.; Hendrickson, D. N.; Fitzgerald, B. J.; Pierpont, C. G.

J.Am.Chem.Soc. 1984, 106, 2041.

14. Sofen, S. R.; Ware, D. C.; Cooper, S. R.; Raymond, K. N. Inorg.Chem. 1979, 18, 234.

15. Connelly, N. G.; Manners, I.; Protheroe, J. R. C.; Whiteley, M. W. J.Chem.Soc. Dalton 1984, 2713.

16. Lynch, M. W.; Valentine, M.; Hendrickson, D. N. J.Am.Chem.Soc. 1982, 104, 6982.

17. Magers, K. D.; Smith, C. G.; Sawyer, D. T. Inorg.Chem. 1980, 19, 492.

18. Griffith, W. P.; Pumphrey, C. A.; Rainey, T-A. J.Chem.Soc. Dalton, 1986, 1125.

19. Buchanan, R. M.; Kessel, S. L.; Downs, H. H.; Pierpont, C. G.; Hendrickson, D. N. J.Am.Chem.Soc. 1978, 100, 7894.

20. Haga, M.; Dodsworth, E. S.; Lever, A. B. P.; Boone, S. R.; Pierpont, C. G. J.Am.Chem.Soc. 1986, 108, 7413.

21. Jones, S. E.; Chin, D-H.; Sawyer, D. T. Inorg.Chem. 1981, 20, 4257.

22. Buchanan, R. M.; Fitzgerald, B. J.; Pierpont, C. G. Inorg.Chem. 1979, 18, 3439.

23. Lynch, M. W.; Hendrickson, D. N.; Fitzgerald, B. J.; Pierpont, C. G. J.Am.Chem.Soc. 1981, 103, 3961.

24. Larsen, S. K.; Pierpont, C. G.; DeMunno, G.; Dolcetti, G.; Inorg.Chem. 1986, 25, 4828.

25. Chin, D-H.; Sawyer, D. T.; Schaefer, W. P.; Simmons, J. Inorg.Chem. 1983, 22, 752.

26. Jones, S. E.; Leon, L. E.; Sawyer, D. T. Inorg.Chem. 1982, 21, 3692.

27. deLearie, L. A.; Pierpont, C. G. J.Am.Chem.Soc. 1986, 108, 6393.

28. Harmalker, S.; Jones, S. E.; Sawyer, D. T. Inorg.Chem. 1983, 22,

2790.

29. Galeffi, B.; Postel, M. Nouv.J.Chim. 1984, 8, 481.

30. Bristow, S.; Enemark, J. H.; Garner, C. D.; Minelli, M.; Morris, G. A.; Ortega, R. B. Inorg.Chem. 1985, 24, 4070.

31. Wilshire, J. P.; Sawyer, D. T. J.Am.Chem.Soc. 1978, 100, 3972.

32. Thompson, J. S.; Calabrese, J. C. Inorg.Chem. 1985, 24, 3167.

33. Mulay M. P.; Garge, P. L.; Padhye, S. B.; Haltiwanger, R. C.; deLearie, L. A.; Pierpont, C. G. J.Chem.Soc. Chem.Commun. 1987, 581.

34. Magnuson, R.H.; Taube, H. J.Am.Chem.Soc. 1975, 97, 5129.

35. Creutz, C.; Chou, M. H. Inorg.Chem. 1987, 26, 2995.

36. Shepherd, R. E.; Proctor, A.; Henderson, W. W.; Myser, T. K. Inorg.Chem. 1987, 26, 2440.

37. (a) Mann, C. K; Barnes, K. K. "Electrochemical Reactions in Non-aqueous Systems", Marcel Dekker, New York, 1970.

    (b) Gritzner, G.; Kuta, J. Electrochim.Acta 1984, 29, 869.

38. Nevin, W. A.; Lever, A. B. P. Anal.Chem. 1988, 60, 727.

39. Stufkens, D. J.; Snoeck, Th. L.; Lever, A. B. P. Inorg.Chem. 1988, 27, 953.

40. (a) Krause, R. A. Inorg.Chim.Acta 1977, 22, 209. (b) Anderson, S.; Seddon, K. R. J.Chem.Res. 1979, 74.

41. Handbook of Chemistry and Physics, 54th Edition, Ed. R. C. Weast, 1973-74, CRC Press.

42. Lever, A. B. P.; Auburn, P. R.; Dodsworth, E. S.; Haga, M.; Liu, W.; Nevin, W. A., to be submitted for publication.

43. Boone, S. R.; Pierpont, C. G., to be submitted for publication.

44. Buchanan, R. N.; Pierpont, C. G. J.Am.Chem.Soc. 1980, 102, 4951.

45. Ref.23 cited in ref.5.

46. Pell, S. D.; Salmonsen, R. B.; Abelleira, A.; Clarke, M.J.

Inorg.Chem. 1984, 23, 385.

47. Stufkens, D. J.; Lever, A. B. P., to be submitted for publication.

48. Bianchini, C.; Masi, D.; Mealli, C.; Meli, A.; Martini, G.;
Laschi, F.; Zanello, P. Inorg.Chem. 1987, 26, 3683.

49. Vlcek, A. A. Electrochim. Acta 1968, 13, 1063.

50. (a) DeSimone, R. E. J.Am.Chem.Soc. 1973, 95, 6238. (b) Sakaki, S.;
Hagiwara, N.; Yanase, Y.; Ohyoshi, A. J.Phys.Chem. 1978, 82, 1917.

   (c) Raynor, J. B.; Jeliazkowa, B. G. J.Chem.Soc. Dalton 1982, 1185.

   (d) Hudson, A.; Kennedy, M. J. J.Chem.Soc. (A) 1969, 1116.

   (e) Lahiri, G. K.; Bhattacharya, S.; Ghosh, B. K.; Chakravorty, A.
   Inorg.Chem. 1987, 26, 4324.

51. (a) Motten, A. G.; Hanck, K. W.; DeArmond, M. K. Chem.Phys.Lett.
1981, 79, 541. (b) Morris, D. E.; Hanck, K. W.; DeArmond, M. K.
J.Am.Chem.Soc. 1983, 105, 3032.

52. Balch, A. L. J.Am.Chem.Soc. 1973, 95, 2723.

53. Girgis, A. Y.; John, Y. S.; Balch, A. L. Inorg.Chem. 1975, 14,
2327.

54. Brown, D. G.; Johnson, W. L. Z.Naturforsch. 1979, 34B, 712.

55. Wicklund, P. A.; Brown, D. G. Inorg.Chem. 1976, 15, 396.

56. Brown, D. G.; Reinprecht, J. T.; Vogel, G. C. Inorg.Nucl.Chem.Lett.
1976, 12, 399.

57. Wilson, H. W. Spectrochim.Acta 1974, 30A, 2141.

58. (a) Srivastava, S. App.Spec.Rev. 1986, 22, 401. (b) Feltham, R. D.;
Brant, P. J.Am.Chem.Soc. 1982, 104, 641. (c) Brant, P.;
Stephenson, T. A. Inorg.Chem. 1987, 26, 22. (d) Connor, J. A.;
Meyer, T. J.; Sullivan, B. P. Inorg.Chem. 1979, 18, 1388.

   (e) Weaver, T. R.; Meyer, T. J.; Adeyemi, S. A.; Brown, G. M.;
   Eckberg, R. P.; Hatfield, W. P.; Johnson, E. C.; Murray, R. W.;

Untereker, D. J.Am.Chem.Soc. 1975, 97, 5039.

59. Perry, W. B.; Schaaf, T. F.; Jolly, W. L. J.Am.Chem.Soc. 1975, 97,
4899.

60. Isied, S. S.; Kuo, G.; Raymond, K. N. J.Am.Chem.Soc. 1976, 98,
1763.

61. Rohrscheid, F.; Balch, A. L.; Holm, R. H. Inorg.Chem. 1966, 5, 1542.

62. Espinet, P.; Bailey, P. M.; Maitlis, P. M. J.Chem.Soc. Dalton 1979,
1542.

63. Sofen, S. R.; Cooper, S. R.; Raymond, K. N. Inorg.Chem. 1979, 18,
1611.

64. Charney, L. M.; Finklea, H. O.; Schultz, F. A. Inorg.Chem. 1982, 21,
549.

65. Anderson, B. F.; Buckingham, D. A.; Robertson, G.B.; Webb,J.
Murray, K. S.; Clark, P. E. Nature 1976, 722.

66. Wilshire, J. P.; Leon, L.; Bosserman, P.; Sawyer, D. T.
J.Am.Chem.Soc. 1979, 101, 3379.

67. Hartman, J. R.; Foxman, B. M.; Cooper, S. R. Inorg.Chem. 1984, 23,
1381.

68. Wicklund, P. A.; Beckman, L. S.; Brown, D. G. Inorg.Chem. 1976, 15,
1996.

69. Gordon, D. J.; Fenske, R. F. Inorg.Chem. 1982, 21, 2907, 2916.

70. Dodsworth, E. S.; Lever, A. B. P. Chem.Phys.Lett. 1986, 124, 152.

71. Heath, G. A.; Yellowlees, L. J.; Braterman, P. S. J.Chem.Soc.
Chem.Commun. 1981, 287.

72. Lever, A. B. P. "Inorganic Electronic Spectroscopy", Elsevier
Science Publishers, New York, 1984, 2nd Edn.

73. Robin, M. B.; Day, P. Adv.Inorg.Chem.Radiochem. 1967, 10, 248.

74. Dallinger, R. F.; Woodruff, W. H. J.Am.Chem.Soc. 1979, 101, 4391.

Table I: A selection of Important Bond Distances and Angles for

Ru(bpy)(Diox)$_2$, (2,5)[a]

Bond distances (Å)		Bond angles (°)	
Ru-O(1)	2.003(4)	O(1)-Ru-O(2)	81.8(1)
Ru-O(2)	1.977(3)	O(2)-Ru-O(3)	94.9(1)
Ru-O(3)	1.995(3)	O(1)-Ru-O(3)	88.0(1)
Ru-O(4)	1.981(3)	O(1)-Ru-O(4)	91.9(1)
Ru-N(1)	2.042(3)	O(2)-Ru-O(4)	173.1(1)
Ru-N(2)	2.055(4)	O(3)-Ru-O(4)	82.0(1)
O(1)-C(1)	1.316(5)	O(1)-Ru-N(2)	173.2(1)
O(2)-C(2)	1.326(6)	O(3)-Ru-N(1)	172.0(2)
O(3)-C(7)	1.322(4)	N(1)-Ru-N(2)	78.2(2)
O(4)-C(8)	1.321(5)		
C(1)-C(2)	1.424(6)		
C(7)-C(8)	1.413(6)		

---

a) R = 0.042, R$_w$ = 0.053 for 2853 reflections. See Figure 1 for numbering scheme.

See Refs. 5 and 20 for X-ray data for Ru(4-t-Bupy)$_2$(DTBDiox)$_2$.

Table II: Electrochemical Data for Ru(bpy)(diox)$_2$ in 1,2-Dichloroethane, $E_{1/2}$ versus SCE[a].

diox	I	II	III	IV	V
DTBDiox	+1.55ir	+0.89	+0.20	-0.82	-1.53qr
Diox	+1.40ir	+1.01qr	+0.37	-0.53	-1.35
TClDiox	+1.54ir	+1.25ir	+0.88	-0.00	-0.95

a) Data recorded against the ferricenium/ferrocene couple as internal calibrant and corrected to SCE by assuming the Fc$^+$/Fc couple lies at +0.31 vs SCE.[37] ir = irreversible; qr = quasi-reversible. The bulk solution is the starting material species (1-5 x 10^{-4} M) with 0.1-0.2 M TBAP as supporting electrolyte. The couples are reversible unless otherwise stated. $E_{1/2}$ values obtained by cyclic and differential pulse voltammetry are essentially identical.

Table III: Electron Spin Resonance Data

Complex	g factors	peak to peak (G)	Conditions
1,R1 [Ru(bpy)(DTBDiox)$_2$]$^{-}$[a]	2.076	92	DCE/RT
	1.937($_{\parallel}$)	35	DCB/77 K
	2.100($_{\perp}$)		
2,R1 Cp$_2$Co[Ru(bpy)(Diox)$_2$]	1.934($_{\parallel}$)	200	solid/77 K
	2.109($_{\perp}$)[b]		
1,O1 [Ru(bpy)(DTBDiox)$_2$]$^{+}$[a]	1.964	210	DCE/RT
	1.985	48	CH$_2$Cl$_2$/77 K
1,O1 [Ru(bpy)(DTBDiox)$_2$]ClO$_4$	1.984($_{\perp}$)	42	solid/77 K
	2.023($_{\parallel}$)		

---

a) Electrochemically generated via bulk electrolysis.

b) Rhombic distortion.

Table IV: Fourier Transform Infrared Spectra - Principal Absorption Bands

Complex	Conditions	Principal Bands[a] (cm^{-1})
2,R1 Cp$_2$Co[Ru(bpy)(Diox)$_2$]	KBr	735, 768, 1253, 1385, 1415, 1464, 1559
1,S Ru(bpy)(DTBDiox)$_2$	KBr	505, 773, 1024, 1099, 1142, 1360, 1375, 1464, 1518, 1583
2,S Ru(bpy)(Diox)$_2$	KBr	527, 728, 743, 772, 1099, 1113, 1208, 1315, 1415, 1448, 1532
3,S Ru(bpy)(TClDiox)$_2$	KBr	767, 798, 979, 1188, 1322, 1384, 1396, 1421
1,O1 [Ru(bpy)(DTBDiox)$_2$]ClO$_4$	Nujol	728, 773, 987, 1027, 1091,[b] 1238, 1339, 1361,[c] 1448,[c] 1466,[c] 1582

a) Only the more prominent peaks are recorded here. Where one or more peaks clearly dominate the spectrum, they are underlined.

b) Hexafluorophosphate salt.

c) Hexachlorobutadiene mull.

Perchlorate absorption, where present, is not reported.

Table V: Photoelectron Emission Data

Complex	Binding Energy[a,b] (eV)		
	Ru($3d_{5/2}$)	O(1s)	N(1s)
2,R1 $Cp_2Co[Ru(bpy)(Diox)_2]$	280.4	—[c]	399.6
1,S $Ru(bpy)(DTBDiox)_2$	280.8	530.7(0.45)	399.7(0.71)
		532.0(0.33)	400.6(0.29)
		533.0(0.21)	
2,S $Ru(bpy)(Diox)_2$	281.3	531.8(0.52)	399.9
		532.4(0.31)	
		533.8(0.19)	
1,O1 $[Ru(bpy)(DTBDiox)_2]ClO_4$[d]	282.0	—[c]	400.5
5,S $[Ru(bpy)_2(DTBSq)]PF_6$	280.8[e]	531.4	399.6(0.44)
			400.9(0.56)

a) Maximum error is ±0.3 eV.

b) Relative intensities in parentheses.

c) Contamination with silicon grease.

d) Perchlorate ion Cl(2p) observed at 207.5(0.64) and 209.1(0.36).

e) Additional signal observed at 281.8 eV believed to be due to differential charging problems. This complex reported in ref. 4.

Table VI: Electronic Spectroscopic Data for Ru(bpy)(diox)$_2$ Redox Series in 1,2-Dichlorobenzene; λ_{max}(nm) (ϵ(L mol^{-1} cm^{-1}))[a]

Species	Color	DTBDiox (1)	Diox (2)	TClDiox (3)
R2	red-brown	865(2950)		
		740(3150)		750br(3500)
		570sh		505sh
		490(8150)		470(8700)
		330sh		
R1	green	850(6600)	ca 780sh	760sh
		695(9200)	680	620(ca 7000)
		430(5150)	400sh	400(ca 5000)
S	deep blue	1175(6050)	1235(4400)	1315(4290)
		955(12100)	955(14400)	1005(16100)
		605(11600)	590(11100)	585(10040)
		505(3100)sh	475(3600)	450sh
		375(5700)	340	420(4140)
O1	violet	720(11100)	720	800(ca 9700)
		505(6550)	515	560(ca 7100)
		390(5700)	590sh	385sh
O2	brown-yellow	950(770)		(b)
		570(3150)		
		390(3220)		

Table VI footnotes

a) Solutions of oxidised and reduced species prepared by controlled potential electrolysis and, in the cases of 1,O1, 1,R1 and 2,R1, also by chemical oxidation or reduction.

b) Solution unstable.

sh = shoulder.

Table VII: Resonance Raman Spectra

Species	Excitation wavelength (nm)	Enhanced frequencies (cm^{-1})
1,S	488	1600, 1550, 1480, 1165, 990, 590, 575, 450
	570	1550, 1475, 1320, 1165, 690, 590vs, 575vs, 535, 505, 490, 450vs, 395, 220, 175, 155
3,S	457.9	1600, 1550, 1485, 565
	580	1520, 1485, 1375, 1125, 810, 615, 565vs, 540, 490, 370, 360, 340, 320, 230, 140
1,01	488 or 514	1495, 1407, 1362, 935, 915, 591, 554vs, 524
	620	1407, 935, 915, 591, 554vs, 524

Spectra were run in 1,2-dichloroethane. Strong bands are underlined and the most strongly enhanced are marked vs.

Table VIII: Summary of Electronic Spectroscopic Assignments

Oxidation State	Species[a]	Wavelength Region (nm)	Assignment
R2	$[Ru(II)(bpy)(cat)_2]^{2-}$	700 - 900	$cat(3b_1)--->bpy(\pi_1{}^*)$
			$Ru(d\pi)--->bpy(\pi_1{}^*)$
		500	$Ru(d\pi)--->bpy(\pi_2{}^*)$
R1	$[Ru(III)(bpy)(cat)_2]^-$	800 - 900	$cat(3b_1)--->bpy(\pi_1{}^*)$
		700	$cat(3b_1)--->Ru(d\pi)(t_{2g}{}^5)$
S	$Ru(II)(bpy)(sq)_2$	900 - 1200	$Ru(d\pi)--->sq(3b_1)$
		600	$sq(n)--->sq(3b_1)$
		500	$Ru(d\pi)--->bpy(\pi_1{}^*)$
O1	$[Ru(II)(bpy)(sq)(q)]^+$	720 - 800	$Ru(d\pi)--->diox(3b_1)$
		570	$diox(n)--->diox(3b_1)$

a) The dominant oxidation state is cited for R1, S and O1 for ease of
assigning the spectra.

Figure Legends

Figure 1

Molecular structure of Ru(bpy)(Diox)$_2$ (**2,S**).$^{+3}$

Figure 2

Cyclic voltammogram of 5.6 × 10^{-4} M [Ru(bpy)(DTBDiox)$_2$]ClO$_4$ (**1,01**) in DCE solution with 0.1 M TBAP. Scan speed = 200 mV s^{-1}.

Figure 3

ESR spectra of (left) [Ru(bpy)(DTBDiox)$_2$]$^-$, (**1,R1**), 1.4 × 10^{-4} M in DCB at 77 K, and (right) [Ru(bpy)(DTBDiox)$_2$]$^+$, (**1,01**), in the solid state at 77 K. The arrows denote the positions of the DPPH signals.

Figure 4

Nujol mull FTIR spectra of A) Ru(bpy)(Diox)$_2$ (**2,S**), B) Ru(bpy)(DTBDiox)$_2$ (**1,S**), C) [Ru(bpy)(DTBDiox)$_2$]PF$_6$ (**1,01**), and D) Cp$_2$Co[Ru(bpy)(Diox)$_2$] (**2,R1**).

Figure 5

Electronic spectra of the redox series based on Ru(bpy)(DTBDiox)$_2$, in DCB solution, prepared by controlled potential electrolysis. The labelling system is explained in the text.

Figure 6

Five orbital model for the (cis) Ru(bpy)(diox)$_2$ redox series. The L(a+b) and d(a+2b) orbitals are arbitrarily ordered within each set. The left hand side of the diagram refers to R2 where E(L) < E(d). Moving

across the diagram covers the range R1, S, O1 and O2 with $E(L) > E(d)$ for O2. The essential features of this qualitative diagram are the crossing of the mainly L and d orbitals, the extensive mixing thereof, and the mainly d nature of the LUMO in R1 compared with mainly ligand in O1 and O2.

Fig 1

V IV III II

2 µA

E, V vs Fc$^+$/Fc

-2.0 -1.5 -1.0 -0.5 0 0.5 1.0

Fig 3

Fig. 4
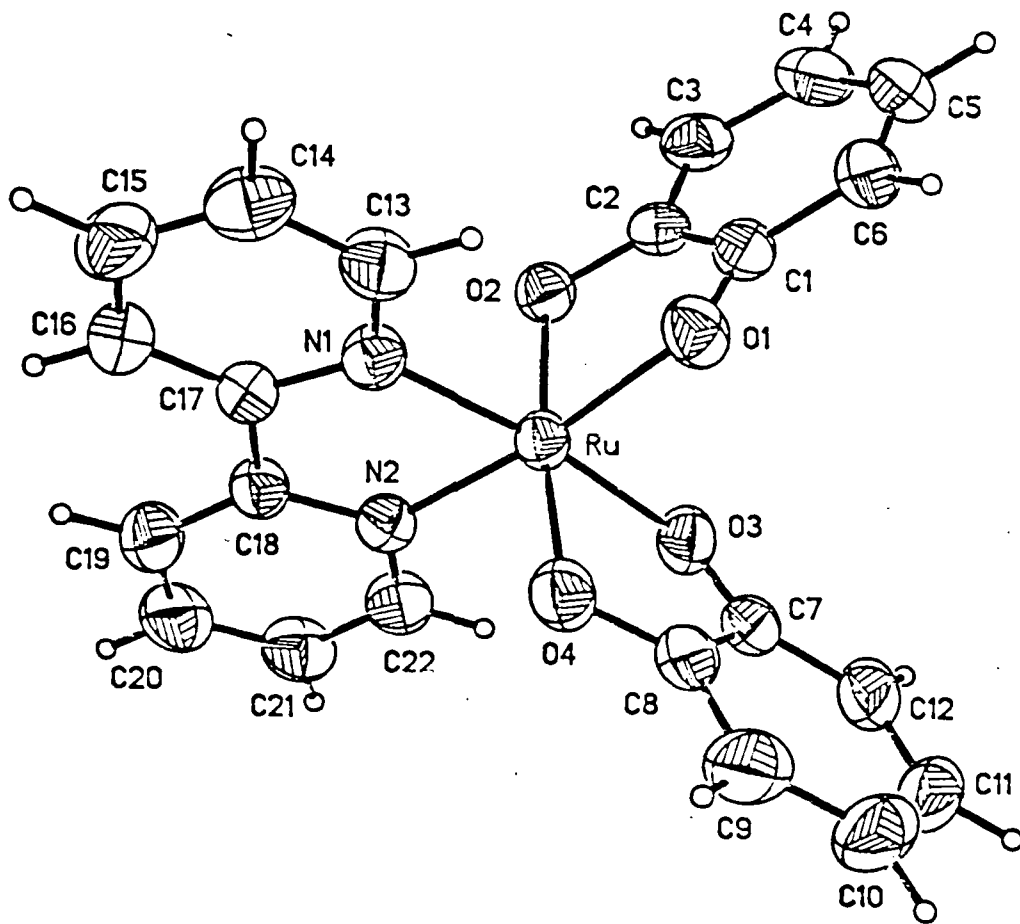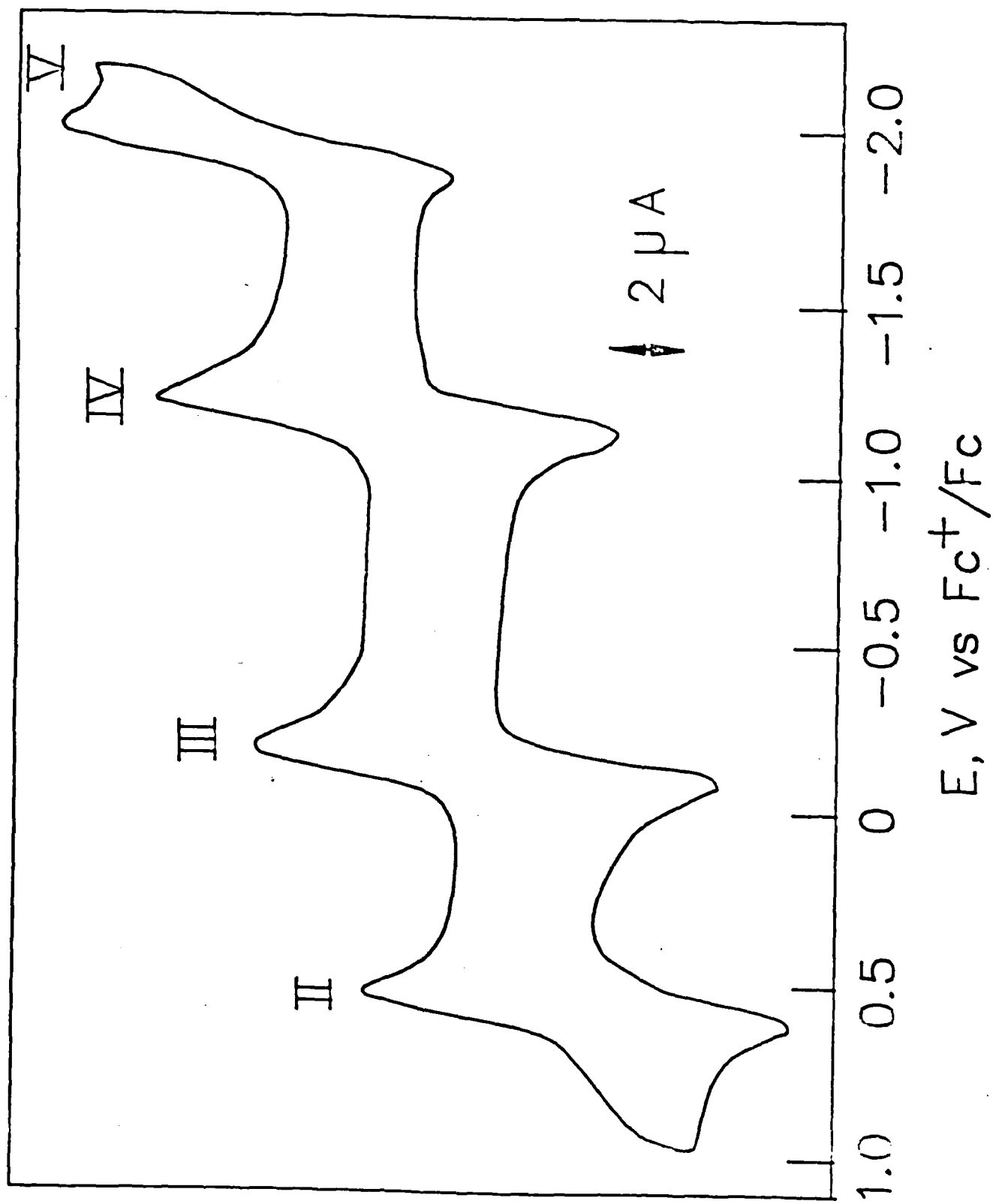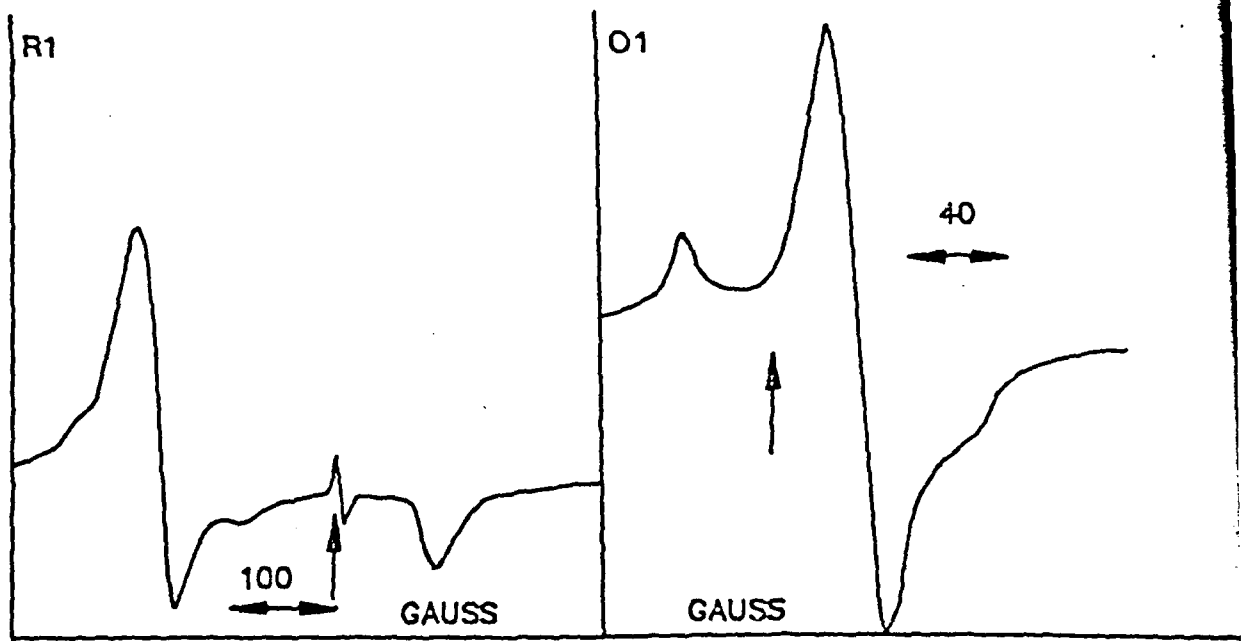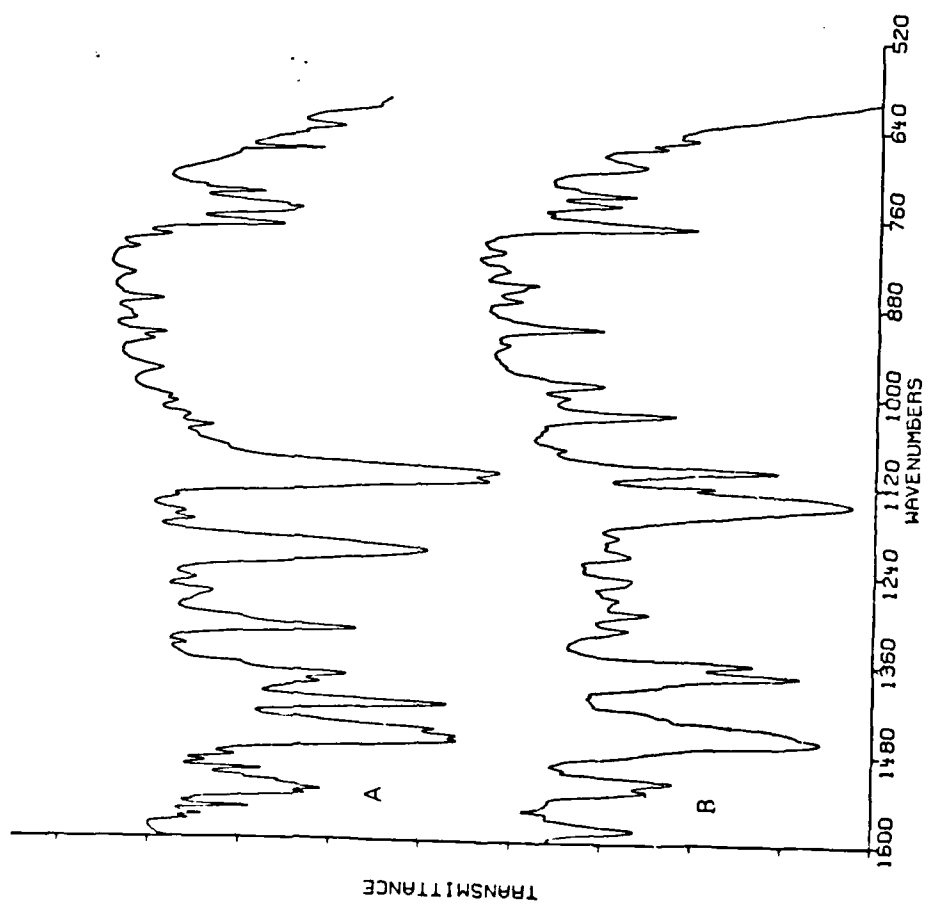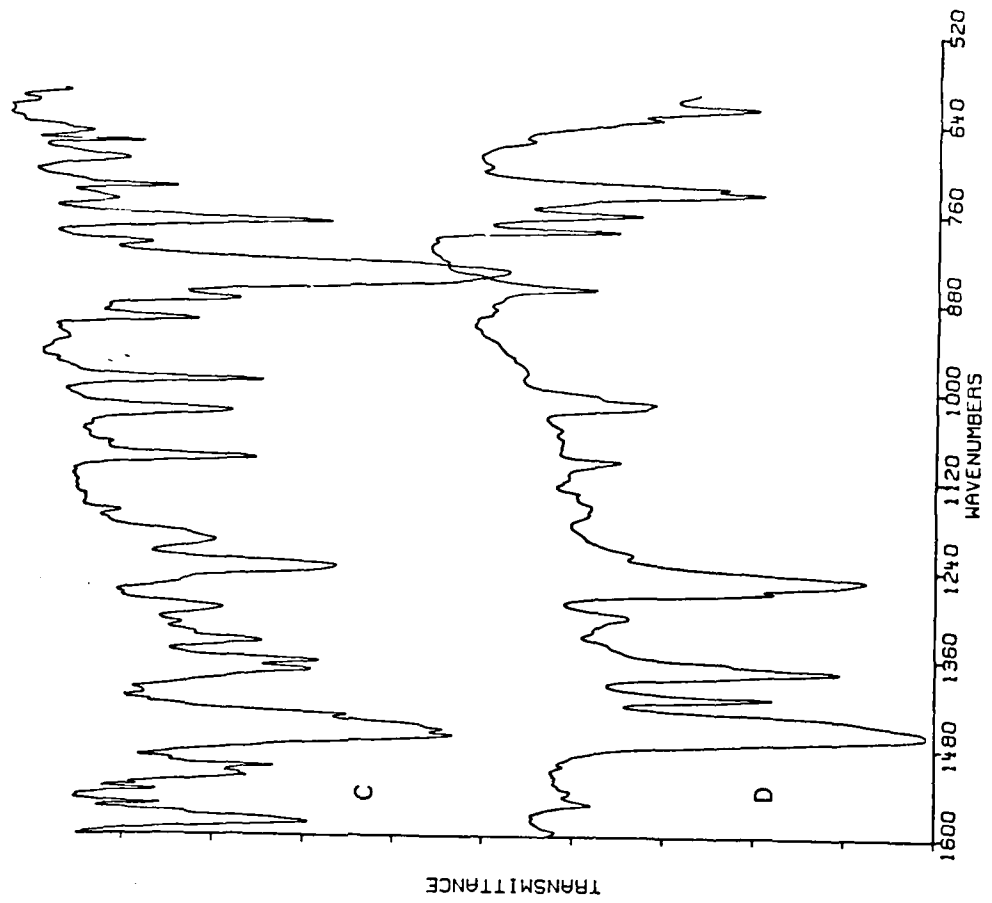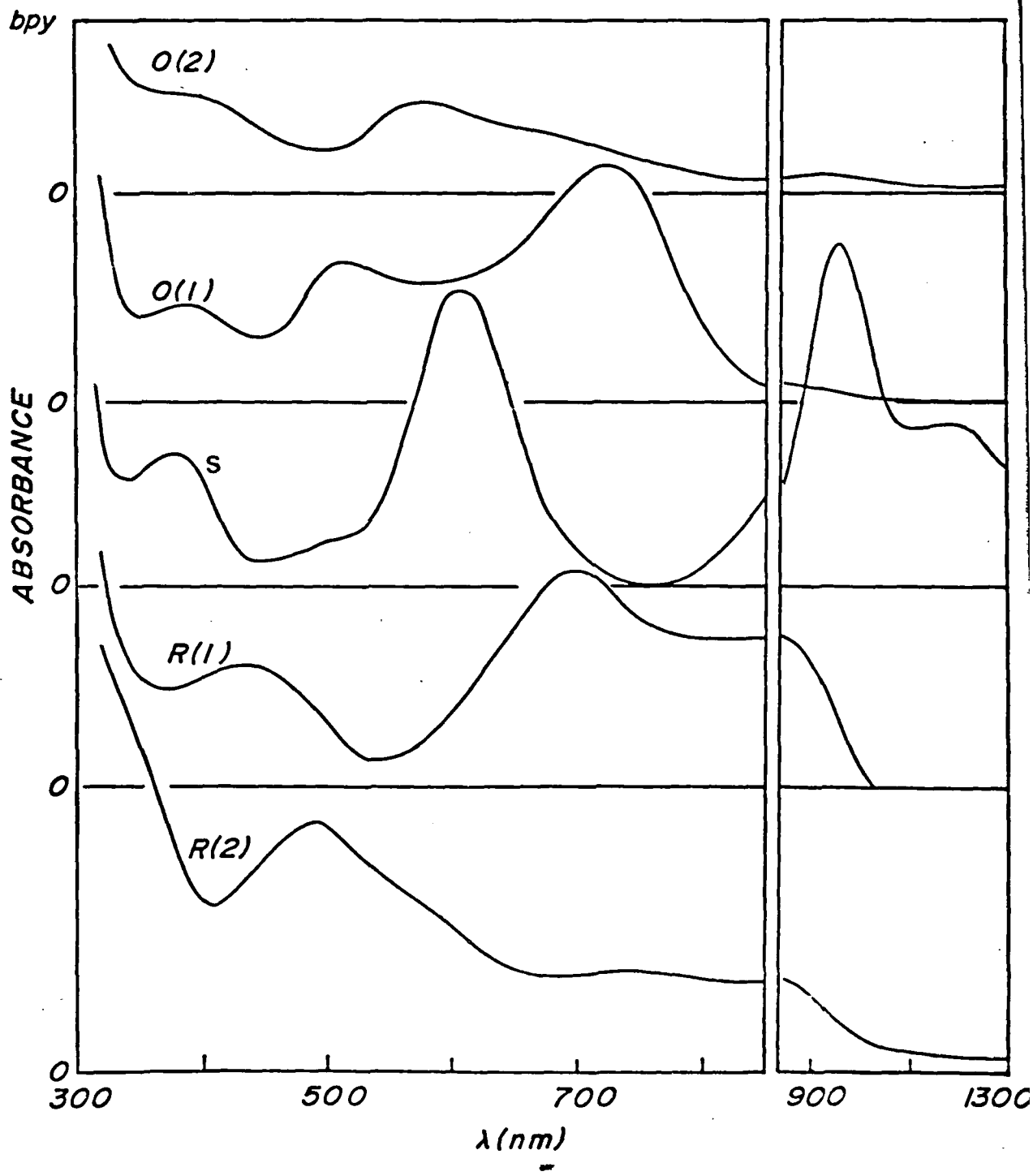
Fig 5

Arbitrary R2 ---- O2 Scale

Arbitrary Energy Scale